Isotope Effects on the Crystallization Kinetics of Selectively Deuterated Poly(ε-caprolactone)

Lengwan Li[1, 2, 4], Dongsook Chang[2], Matthias M. L. Arras[3], Wei Li[2], Tianyu Li[2, 5], Jong K. Keum[2, 3], Peter V. Bonnesen[2], Xiangfang Peng[1]*, Kunlun Hong[2, 4]*

[1] *The Key Laboratory of Polymer Processing Engineering of Ministry of Education, South China University of Technology, Guangzhou 510640, China*

[2] *Center for Nanophase Materials Sciences and* [3] *Neutron Scattering Division, Oak Ridge National Laboratory, Oak Ridge, Tennessee 37831, USA*

[4] *Department of Chemical and Biomolecular Engineering and* [5] *Department of Materials Science and Engineering, University of Tennessee, Knoxville, Tennessee 37996, USA*

Correspondence to:

Xiangfang Peng (pmxfpeng@scut.edu.cn);

Kunlun Hong (hongkq@ornl.gov).

Abstract:

Deuterium labeling of semi-crystalline polymers can dramatically affect their crystallization behaviors. However, the influence of different labeled positions in a partially deuterated polymer on its crystallization is still far from understood. Here, we synthesized a series of selectively deuterated PCLs through ring-opening polymerization of ε-caprolactone with controlled deuteration sites, including fully protiated (D0), fully deuterated (D10), tetra deuteration at the 3- and 7- caprolactone ring positions (D4) and hexa deuteration at the 4-, 5- and 6-caprolactone ring positions (D6). All the PCLs showed a similar lamellar structure and parameters. Differential scanning calorimetry (DSC) analysis revealed that the equilibrium melting temperature T_m^0, melting temperature T_m, crystallization temperature T_c, and crystallization kinetics changed systemically with the deuterium content except for D4, which indicates that the presence of $–CD_2–$ moieties near ester group in the polymer chain combining with isotopically inhomogeneous could influence the chain packing processing. The non-monotonic trend of T_m as a function of deuterium content could possibly be attributed to the difference in a hydrogen-bond like intermolecular interaction between different PCLs. Partially deuterated PCLs (D4 and D6) showed an Avrami index near 2. After analyzing the parameters at the same supercooling temperature ΔT_c, the existence of two crystallization regimes of PCLs were detected.

Table of Contents (TOC) Graphic

Deuterium substitution of semi-crystalline polymers can dramatically affect their crystallization behavior. Four types of deuterated poly(ε-caprolactone) (PCL) with controlled deuteration sites are investigated by SANS and DSC measurements. It is observed that crystallization kinetics is sensitive to the nature of the deuteration sites and the crystallization kinetics of partially deuterated PCLs do not always show deuterium content dependence. Partially deuterated PCLs were also found to reveal different growth manner.

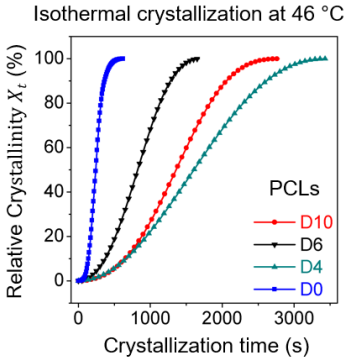

For Table of Contents use only

INTRODUCTION

The replacement of protium (H) with deuterium (D) at selected positions is a very useful method for elucidating the dynamics and structures in polymeric materials. A number of studies have been carried out using deuterated polymers as a molecular probe. For examples, Knauer et al. labeled the chain ends of polyethersulfone (PESU), to locate the accurate position of chain ends in PESU thin film-air interface.[1] Chen et al. investigated the mechanism of liquid-liquid phase separation in random ethylene 1-hexene copolymer by adding deuterium to certain fraction.[2, 3] Deuterated polyethylene (PE) was proved to be the key in elucidating the shish-kebab superstructures and chain alignment of PE under cold-draw through small-angle neutron scattering (SANS).[4, 5] Concurrently, various methods for the synthesis of deuterated polymers has been reported, including polymerizing the deuterated monomers,[6] saturating polydienes with deuterium gas (D_2), and introducing deuterium at elevated pressure and temperature over different heterogeneous catalysts in the presence of D_2.[7-9] However, D substitution technique sometimes exhibits non-subtle isotope effect, such as different crystallization kinetics, which implicates the usage of D labeling in rigorously controlled crystallization studies.[10, 11] For example, different crystallization kinetics between H and D species could result in separated H and D crystal domains instead of co-crystal during the slowly cooling process from the melt.[12] Herein, a fundamental understanding of the difference between the crystallization behavior of H- and D- polymer is important for the studies using the D substituted chain as a probe for characterization.

The impact of deuterated polymer chains on the crystallization behaviors has been studied since the 1970s by many researchers, including Stehling, Bates, and Wignall,[11-13] with main focus on polyolefins, one of their conclusion was that deuterated polyolefins with heavier mass would have a slower kinetics than protiated polyolefins. Moreover, recent usage of deuterium labeling produced some extra interesting phenomenon that have attracted researchers' attention. For instance, Tashiro et al. found that at the same supercooling temperature (ΔT_c), H/D blends of isotactic polypropylene (iPP) with higher D content had a higher crystallization rate,[14] whereas H/D polyoxymethylene (POM) blends showed an opposite trend.[15] Habersberger et al. reported that a partially deuterated syndiotactic polypropylene (sPP) with statistical H/D distribution displayed a 12.5 °C reduction in melting point, suggesting the possibility that partial deuterium substitution is more disruptive to the crystal

structure than full substitution.[7] Jakowski et al. reported the orders in the crystallinity of the poly(3-hexylthiophene)s (P3HT) with different substitution is P3HT-D0 > P3HT-D13 (side-chain dueteration) > P3HT-D1 (main-chain deuteration) > P3HT-D14, the opposite trend (P3HT-D13 > P3HT-D1) demonstrated that the reduced crystallinity of main-chain deuteration is not caused by the slower crystallization kinetics because of the increased mass of deuterated P3HTs.[16] These new findings show the need of a detailed investigation of deuteration effect on the crystallization behaviors in partially deuterated polymers.

In the present paper, the crystallization behavior of poly(ε-caprolactone) (PCL) with different deuteration levels was investigated to ascertain the effects of deuteration. PCL, a semi-crystalline polyester, is widely used in industrially relevant processes (e.g., the manufacture of polyurethanes) and also in high-tech areas, such as biomaterials and 3D-printing. Selectively deuterated PCLs were synthesized by ring-opening polymerization of ε-caprolactone with precisely controlled deuteration positions and thoroughly characterized. Four types of PCLs (i.e., $-(C_6D_xH_{10-x}O_2)_n-$, with x = 0, 4, 6, and 10), denoted as fully protiated (D0), fully deuterated (D10), tetra deuterated at the 3- and 7- ring positions (D4), and hexa deuterated at the 4-, 5-, and 6- ring positions (D6), were examined. Crystallization of these PCLs were investigated by SANS and differential scanning calorimetry (DSC). Experimental data regarding crystal morphology, equilibrium melting temperature T_m^0, melting temperature T_m, crystallization temperature T_c, and crystallization kinetics were obtained. Avrami model were adopted to analyze the data.

EXPERIMENTAL SECTION

Materials

All reagents were used as received from the suppliers without further purification unless otherwise noted. Cyclohexanone-d_{10} (Lot PR-27303B; nominally~98 atom %D) was received from Cambridge Isotopes Laboratories, Inc. By ^{13}C NMR analysis the actual deuterium distribution was found to be ~94 atom %D at the carbons α to the carbonyl (with a $–CD_2–$ to –CDH– ratio of about 88:12), and ≥98 atom % at the β-carbons and at the γ-carbon. The solvents were purchased from Fisher Scientific.

Sample Preparation

Fully deuterated ε-caprolactone-d_{10} (CL-d10) and partially deuterated ε-caprolactone-d_4 (CL-d4) were synthesized through the Baeyer-Villager oxidation as reported in our recent study.[6] To achieve a better transition of the degree of deuteration from 0%, to 40%, to 60%, and then to 100%, ε-caprolactone-d6 (CL-d6), which is shown in Figure S1 was synthesized in this work (described below). It is worth mentioning that the CL-d6 has an opposite deuteration structure compared with CL-d4, that is, the protons in CL-d4 are deuterons in CL-d6 while the deuterons in CL-d4 are exchanged to protons in CL-d6.

Synthesis of 3,3,4,4,5,5-hexadeuterocyclohexanone.

Cyclohexanone-d_{10} (22.73 g, 0.21 mol) was diluted with a mixture of THF (30 mL) and dichloromethane (10 mL) in a 250-mL round-bottom flask. To this solution was added 25 g of 0.5 M potassium carbonate in distilled deionized water, and the rapidly stirred mixture was heated in a 68 ºC oil bath for 18 h. The mixture separated into two phases upon cooling, and a 50 μL aliquot from the upper organic phase was diluted with 700 μL $CDCl_3$. ^1H and ^{13}C NMR analysis revealed the cyclohexanone to be about 39-40 atom %H at the 2- and 6-positions, indicating the theoretical exchange equilibrium was slightly more than half complete. The ratio CH_2:CDH:CD_2 carbons was 1.0 (singlet at 41.86 ppm) : 4.2 (triplet centered at 41.53 ppm) : 2.6 (pentet centered at 41.20 ppm). Heating was continued for an additional 22 h, with NMR analysis showing the cyclohexanone to be about 61 atom %H at the 2- and 6-positions. The ratio CH_2:CDH:CD_2 carbons was now 1.0 : 1.6 : 0.35. The phases were separated and the aqueous phase was extracted with dichloromethane (2 x 30 mL). The dichloromethane extracts

were combined with the organic phase and returned to the flask along with ca. 10 mL THF, and 29 g of fresh 0.5 M potassium carbonate in Milli-Q water. About 2/3 of the dichloromethane was removed by rotary evaporation, and the remaining mixture then was heated as before for 48 h. NMR analysis revealed the cyclohexanone to now be about 88 atom %H at the 2- and 6-positions, with the ratio CH_2:CDH:CD_2 carbons now 1.0 : 0.32 : 0 (not detected). The workup and exchange procedure was repeated a third time (ca. 95 atom% H) and then a final time, affording 96-97 atom %H overall. The final organic solution was dried through a column of anhydrous granular sodium sulfate and diluted with additional dichloromethane to a total mass of 280 g (about 215 mL total volume). NMR analysis of this solution indicates that recovery is ca. 78%. This solution was then used in the subsequent step. ^{1}H NMR ($CDCl_3$): δ 2.28 (br s, –CH_2–), 2.26 (br s, residual alpha –CDH– integrating at about 3-4%). ^{13}C{^{1}H} NMR ($CDCl_3$; pw = 45, d1 = 20 sec): δ 212.4 (CO from residual –CDH– material), 212.3 (CO from CO from –CH_2– material),), 41.9 (s, –*C*H_2C(O)*C*H_2–, at ~97%), 41.5 (t, J_{CD} = 20 Hz, –*C*HD– at ~3%), 26.1 (p, J_{CD} = 19.6 Hz, beta –CD_2–), 23.9 (p, J_{CD} = 19.3 Hz, gamma –CD_2–).

Synthesis of 2-Oxepanone-4,4,5,5,6,6-d6 (ε-caprolactone-d6)

The solution from above containing 3,3,4,4,5,5-hexadeuterocyclohexanone in ca. 215 mL CH_2Cl_2 was combined in a 2-L flask with Bi(III) triflate (6.56 g, 10.0 mmol), and diluted with additional dry CH_2Cl_2 (435 mL). The flask was cooled in an ice bath under nitrogen flow, and a suspension of *meta*-chloro-peroxybenzoic acid (*m*-CPBA, 72 g at 70-75% purity) in 150 mL dry CH_2Cl_2 was added. The reaction was conducted in the same manner as in our previous study[6] for ε-caprolactone-d10 with the exception that saturated aqueous Na_2SO_3 was employed in place of saturated aqueous $Na_2S_2O_3$ during the workup. The crude ε-caprolactone-d_6 was purified by fractional vacuum distillation from powdered calcium hydride (CaH_2). The yield on the high purity center cut distilling at 59-61 ºC at ca. 0.6 Torr was 16.8 g (67% overall yield from cyclohexanone-d_{10}). This fraction had a chemical purity of ≥99% and was ca. 96-97 atom %H at the 3 and 7 positions. The monomer was stored frozen under nitrogen until ready to use. ^{1}H NMR ($CDCl_3$): δ 4.15 (br s, 2H, –CH_2–OC(O)–), 2.55 (br s, 2H, CH_2–C(O)–). ^{13}C{^{1}H} NMR ($CDCl_3$; pw = 45, d1 = 20 sec): δ 176.3 (CO), 69.2 (s, –O*C*H_2– at ca. 94%), 69.0 (t, J_{CD} = 22 Hz, residual –O*C*HD– at ca. 6%), 34.3 (s, –*C*H_2C(O)– at ca 93%), 33.9 (t, J_{CD} = 20 Hz, –*C*HDC(O)– at 7%),

28.3 (p, J_{CD} = 19 Hz, –$OCH_2CD_2CD_2$– at ~99%), partially overlaps with 27.7 (p, J_{CD} = 20 Hz, –$OCH_2CD_2CD_2$– at ~99%D), 22.0 (p, J_{CD} = 20 Hz –$CD_2CH_2C(O)$– at ~99%).

PCL polymers were synthesized by ring-opening polymerization of the ε-caprolactone monomer as shown in Figure S1. All of the PCL blends were prepared by solution blending of the respective polymer in chloroform solutions.

Sample Characterization

^1H and ^{13}C NMR spectra were obtained on a Varian VNMRS 500 NMR spectrometer at 23°C in $CDCl_3$ (7.27 ppm ^1H reference and 77.23 ppm ^{13}C reference). Carbon NMR spectra were obtained using inverse-gated decoupling with pw = 90 and a recycle delay of 60 seconds, unless otherwise noted. The average acquisition is about 1000 scans. The number average molar mass (M_n) and dispersity of polymers were measured with a size exclusion chromatography (SEC) system equipped with an Agilent 1260 infinity Isocratic HPLC pump, a multi-angle light scattering detector (DAWN HELEOS-II, Wyatt), and a refractive index detector (Optilab T-rEX, Wyatt). THF was the eluent (1 mL/min, at 35 °C). Absolute molar masses were calculated with the dn/dc values measured separately (Table 1).

The polymers for SANS measurements were sandwiched between a pair of quartz plates with a 0.5 mm thickness aluminum split-ring washer and the procedure was carried out on a Linkam hot stage (THMS600) at 90 °C. Then, the sandwiched polymers were loaded to a Titania cell. The SANS were performed at the Bio-SANS instrument at the High-Flux Isotope Reactor, Oak Ridge National Laboratory. The sample-to-detector distance was set to 15.5 m with a wavelength of 6 Å and wavelength spread $\Delta\lambda/\lambda$ = 0.13. The available q range was 0.003 < q < 0.8 A^{-1}, where $q = (4\pi\ sin\theta)/\lambda$, and 2θ is the scattering angle. Raw SANS data were corrected for sample transmission and background radiation.

Differential scanning calorimetry (DSC) was carried on a Q-2000 DSC (TA Instruments) equipped with an RCS90 air cooler. All the tests were performed under nitrogen protection and the instrument was calibrated with the order of sapphire standard, indium standards, and empty cell. Polymer powders were loaded into aluminum hermatic pans. Each sample was first heated to 80 °C and equilibrated for 10 min to erase thermal history.

RESULTS AND DISCUSSION

Synthesis results

Four ε-caprolactone monomers with different deuteration levels were synthesized and designated as d0, d4, d6 and d10, respectively, as shown in Figure 1 along with their corresponding ^{13}C NMR spectra measured in $CDCl_3$ solution. As seen in the spectra, five peaks were observed at all the CD_2 unit positions due to the spin-spin couplings between ^{13}C and D atoms. The isotopic purity of each CD_2 and CH_2 unit is over 96%. PCLs were synthesized from these monomers through ring-opening polymerization and the ^{13}C NMR are shown in Figure S2. Synthesized D0, D4, D6 and D10 polymers (Figure 2a) with similar molar mass and distributions were chosen for this work, as listed in Table 1. SEC traces of the PCLs in Figure 2b show their hydrodynamics sizes in THF closely to each other.

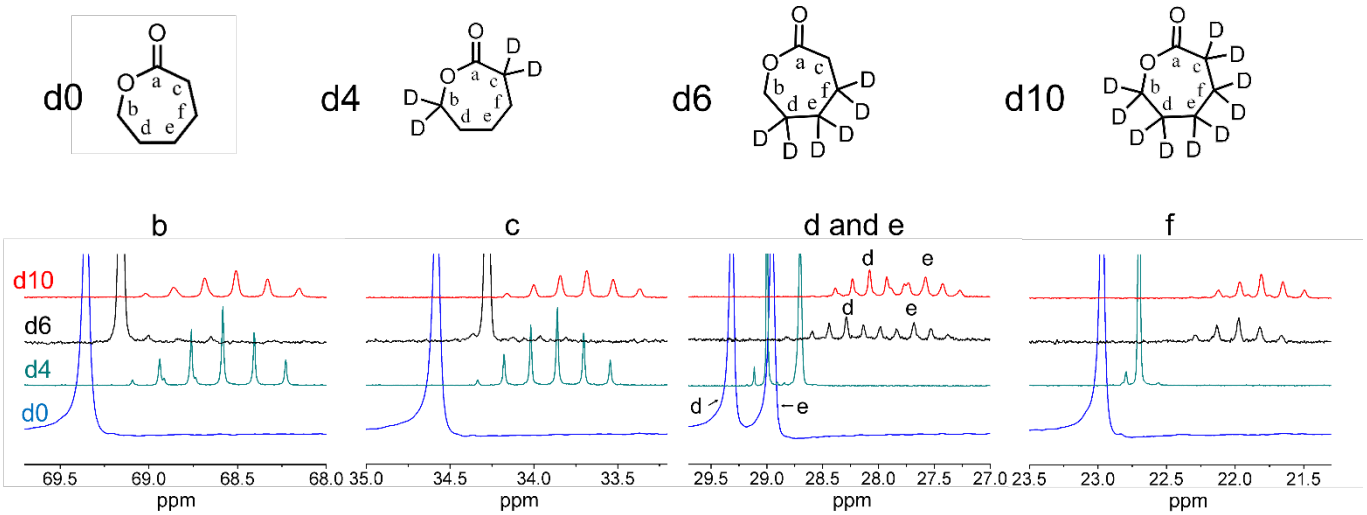

Figure 1. Structure and ^{13}C NMR of d0, d4, d6, d10 monomer.

Table 1. Information of synthesized polymers.

Polymers	M_n (g/mol)	dn/dc[a]	Molar mass per unit (g/mol)	Degree of polymerization	Dispersity
D10	11,700	0.052	124.21	95	1.16
D6	9,700	0.058	120.18	81	1.16
D4	10,700	0.061	118.17	92	1.35
D0	10,900	0.067	114.14	96	1.29

[a]dn/dc of D6 are estimated based on the values in D0, D4 and D10.

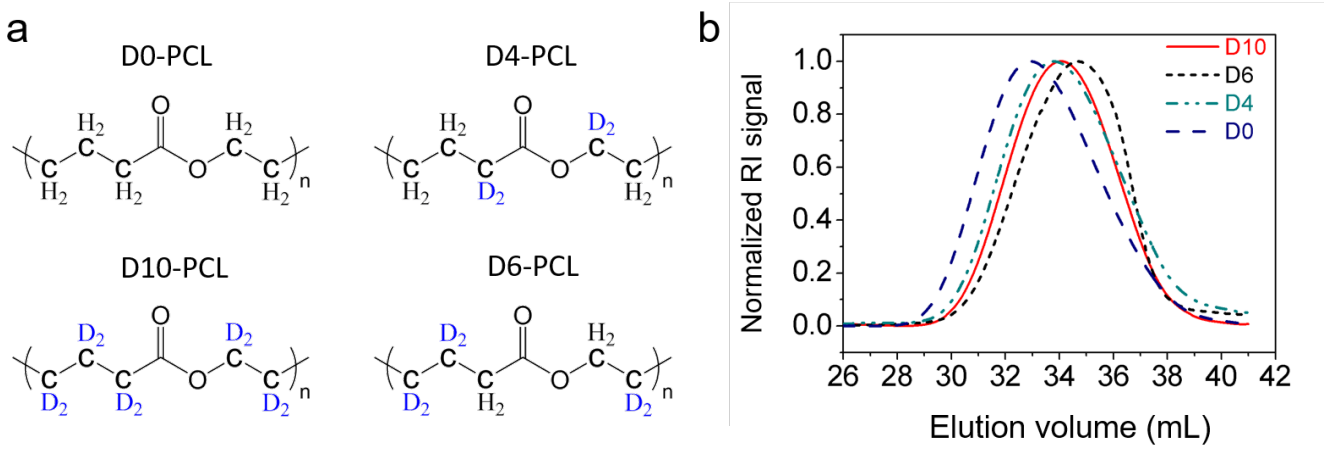

Figure 2. (a) Structures of PCLs and (b) SEC traces of PCLs obtained in THF.

Crystallization behavior

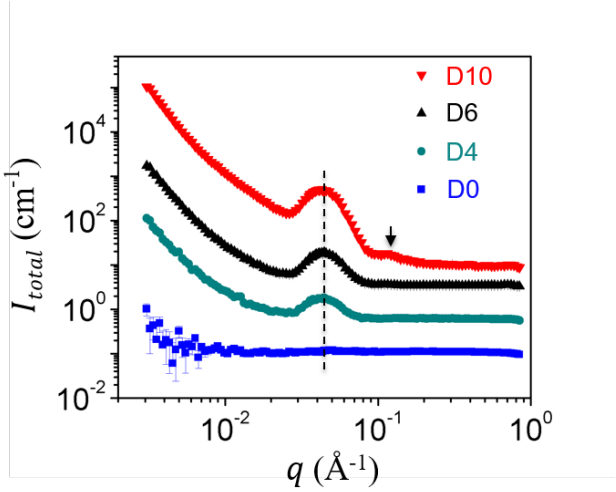

Figure 3. SANS measurements of total scattering intensity I_{total} vs. q of D0, D4, D6 and D10 PCL samples (from bottom to top). Curves were vertical shifted for clarity.

SANS experiments were conducted to investigate the crystal morphology of PCLs. Figure 3 showed the total scattering intensity I_{total} as a function of scattering vector q from SANS for PCLs. One finds that with increasing the deuteration ratio, the lamellar peak becomes larger due to the enhancement of coherent scattering intensity. The D10 sample showed a tiny secondary peak (indicated by arrow), which is attributed to the second order. Other samples may have similar second order, however, the signal was shielded by the incoherent scattering of H content.

The peak positions of the scattering curves are around 0.044 Å^{-1}, suggesting the same lamellar parameters of all PCLs.

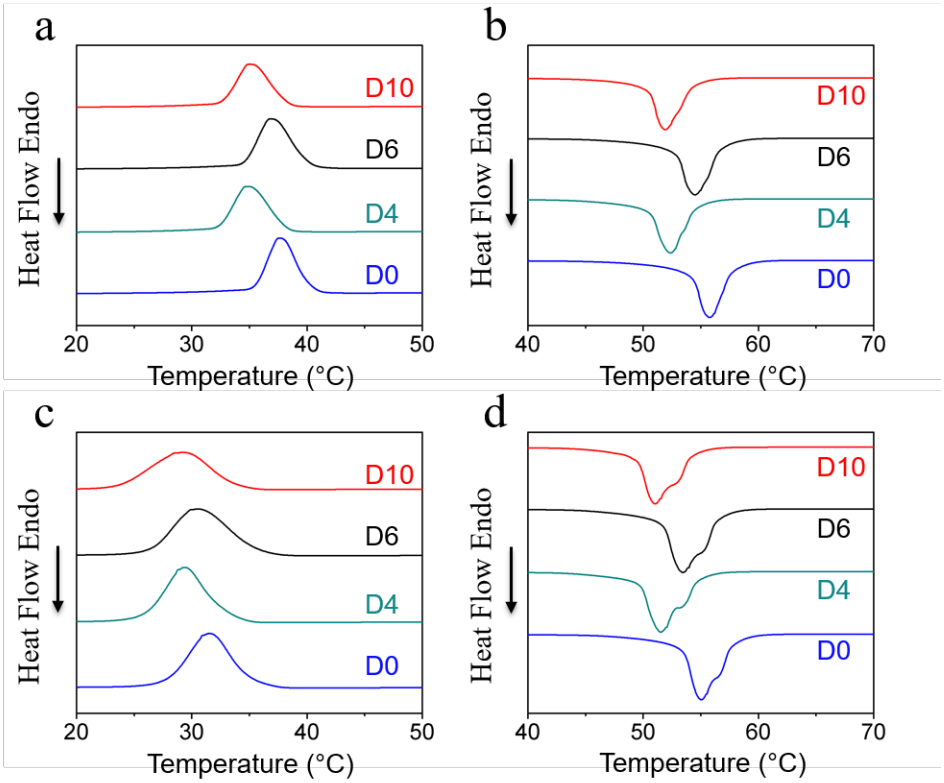

Figure 4. DSC results: (a) cooling curves at rate 2.5 ºC/min from the melt, (b) subsequent heating curves at rate 10 ºC /min, (c) cooling curves at rate 10 ºC/min from the melt and (d) subsequent heating curves at rate 10 ºC /min of D0-, D4-, D6- and D10-PCL samples (from bottom to top). Curves are vertically offset for clarity.

The melting and crystallization behavior of selectively deuterated PCLs was examined using DSC. The thermograms in Figures 4a and 4c show the results from slow cooling (2.5 ºC/min) process and relatively rapid cooling (10 ºC/min), respectively. While the subsequent heating curves are presented in Figures 4b and 4d. These calorimetry results are summarized in Table 2. D10 sample exhibits lower T_m and T_c than D0, while D6 shows intermediate values of T_m and T_c between D10 and D0. In general, T_m and T_c decreases with increasing deuterium content. T_m showed a relationship of T_m(D0) > T_m(D6) > T_m(D4) > T_m(D10). Melting point and crystallization temperature depression of deuterated polymers has been reported by lots of studies.[7, 13] However, the T_m of D4, lower than that of D6, does not follow this trend. The slightly larger dispersity of D4 seems not to

be the reason for the lower melting temperature, according to the normal DSC peak shape of D4. We expect that D atoms in different deuteration sites could lead to different changes of a specific intermolecular interaction, which affect the melting temperature. Detailed analysis will be presented in a later section.

Table 2. Melting temperature (T_m), crystallization temperatures (T_c), and equilibrium melting temperature T_m^0 from calorimetry measurements (T_m and T_c are obtained from the peak maximum. Difference between deuterated and protiated PCLs is reported in parentheses).

Polymers	cooling rate 2.5 °C/min		cooling rate 10 °C/min		T_m^0 (°C)
	T_m (°C)	T_c (°C)	T_m (°C)	T_c (°C)	
D10	52.0 (-3.9)	35.2 (-2.6)	51.1 (-4.0)	29.4 (-2.2)	74.6 (-5.6)
D6	54.5 (-1.4)	36.9 (-0.9)	53.5 (-1.6)	30.7 (-0.9)	79.0 (-1.2)
D4	52.4 (-3.5)	34.8 (-3.0)	51.5 (-3.6)	29.4 (-2.2)	75.9 (-4.3)
D0	55.9	37.8	55.1	31.6	80.2

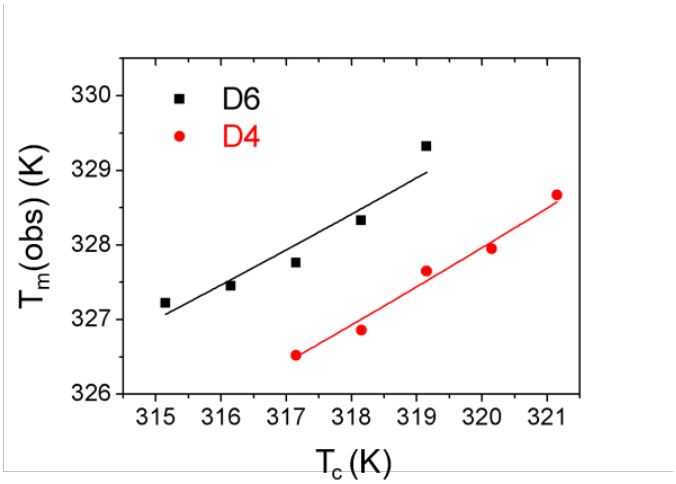

Figure 5. Observed T_m as a function of isothermal crystallization temperature T_c for D4 and D6 PCLs, the lines were fitted through modified Hoffman−Weeks equation.

Another important thermodynamic parameter for the polymer melt-crystallization study is equilibrium melting temperature T_m^0. Attention is herein focused on estimating the T_m^0 value of PCLs. An indirect procedure was employed using the modified Hoffman-Weeks method[17] as shown in Figure 5. From DSC, the values of observed

melting point T_m(obs) were evaluated as a function of isothermal crystallization temperature T_c. The data points were then fitted through a modified Hoffman-Weeks equation[17] to extract the T_m^0 of D4 and D6. The equation is listed below:

$$T_m = T_m^0 \left[1 - \frac{2\sigma}{\Delta h^0 \beta \left[\frac{2\sigma T_m^0}{\Delta h^0 (T_m^0 - T_c)} + \delta L_c \right]} \right] \quad (1)$$

where σ is the fold surface free energy, Δh^0 is the heat of fusion at T_m^0, β is the crystal thickening factor, and δL_c is the difference between virgin crystal and minimum crystal thickness. T_m^0 is the only variable for fitting with the parameter setting[17]: σ=0.09 Jm^{-2}, Δh^0=1.63×10^8 Jm^{-3}, β=1 and δL_c=5nm. This equation faithfully captures the trend of the overall data, as the differences between fitted curves and data points were less than 0.3K. Herein, we extracted T_m^0 for D4 and D6 and summarized the values in Table 2, while the T_m^0 of D0 and D10 samples were taken from our previous work.[6] The T_m^0 values of PCLs show the same trend as the T_m: T_m^0(D0) > T_m^0(D6) > T_m^0(D4) > T_m^0(D10).

The Avrami model, which is commonly used to describe isothermal crystallization kinetics of polymers,[18, 19] was adopted to study the crystallization process of PCLs at various T_c. In the analysis, the induction time t_0 for the nuclei formation was removed from the isothermal crystallization time. Crystallinity X_t was calculated through the integration of exothermic peak over the crystallization processing. For comparison, the D0/D10 blends with blending ratio of 6/4 and 4/6 were also prepared. Examples of X_t as a function of crystallization time t at T_c = 46°C are shown in Figures 6a and 6b for selectively deuterated PCLs and D0/D10 blends, respectively. From the figure, the half crystallization time $t_0 + t_{1/2}$, which is defined as the time needed to achieve 50% crystallinity, can be determined. In Figure 7, we present the induction time t_0 and half crystallization time $t_0 + t_{1/2}$ for isothermal crystallization at various temperatures. It is manifest that the crystallization process become slower as T_c increases. For D0/D10 blends, t_0 and $t_0 + t_{1/2}$ increase continuously with increasing the D content.

By contrast, partially deuterated PCLs does not follow the same trend, and in particular, D4 displayed the largest t_0 and $t_0 + t_{1/2}$ among all the samples.

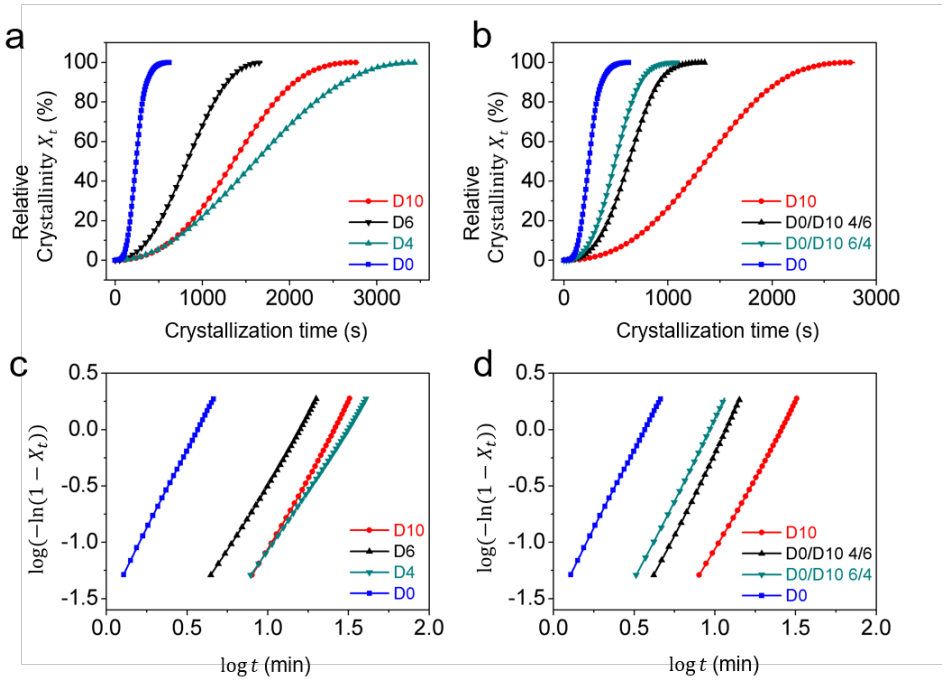

Figure 6. Relative crystallinity X_t as a function of crystallization time t at T_c = 46 °C for (a) selectively deuterated PCLs and (b) D0/D10 blends; Avrami plots at T_c = 46 °C for (c) selectively deuterated PCLs and (d) D0/D10 blends.

Attention is focused on the crystallization phenomenon of D4. The Avrami equation assumes that X_t is related to the crystallization time as:[20-22]

$$X_t = 1 - \exp\left[-k(t)^n\right] \qquad (2)$$

where n is the Avrami index and k is the crystallization rate constant. Equation 2 can be rewritten as:

$$\log\left[-\ln(1 - X_t)\right] = \log k + n \log t \qquad (3)$$

From Figure 6c and 6d, n and log k were extracted from the linear fit of $\log\left[-\ln(1 - X_t)\right]$ versus log t for X_t from 0.05 to 0.85, which are listed in Table 3 and Table S1, respectively. Avrami index n corresponds to the crystal growth dimension, n = 3 suggests the disk-like growth for homogeneous crystallization, n = 2 indicates rod-like growth from sporadically generated nuclei (homogeneous crystallization) or disk-like growth from

already existing nuclei (heterogeneously crystallization)[14]. In Table 3, D0, D10, and the blends show n values close to 3, whereas D4 and D6 show n values close to 2, indicating that selectively deuterated PCLs may go through a different crystallization process.

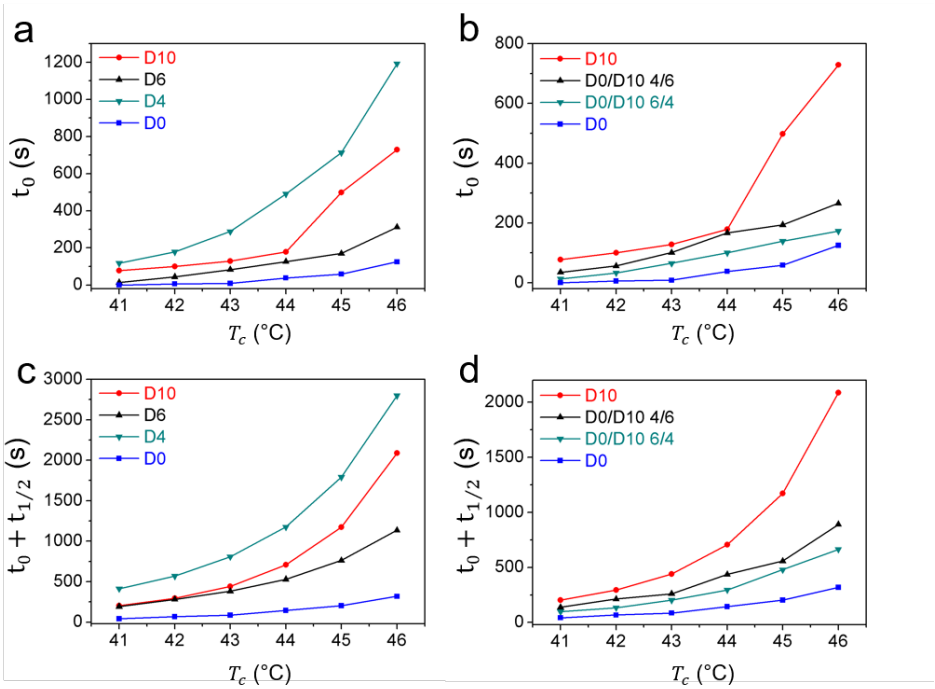

Figure 7. (a) Induction time t_0 and (c) half crystallization time $t_0 + t_{1/2}$ for selectively deuterated PCLs after isothermal crystallization at 41-46 °C; (b) Induction time t_0 and (d) half crystallization time $t_0 + t_{1/2}$ for D0/D10 blends after isothermal crystallization at 41-46 °C. The data point values are presented in Table S1.

Table 3. Avrami index n, obtained for PCLs at different isothermal crystallization temperature T_c

Temperature (°C)	D0	D0/D10 6/4	D0/D10 4/6	D10	D4	D6
46	2.78	2.89	2.95	2.60	2.18	2.41
45	2.75	2.76	2.86	2.51	2.20	2.35
44	2.74	2.65	2.86	2.91	2.09	2.31
43	2.67	2.45	2.47	2.80	2.16	2.30
42	2.94	2.66	2.81	2.66	2.16	2.27
41	2.48	2.72	2.52	2.56	2.17	2.18

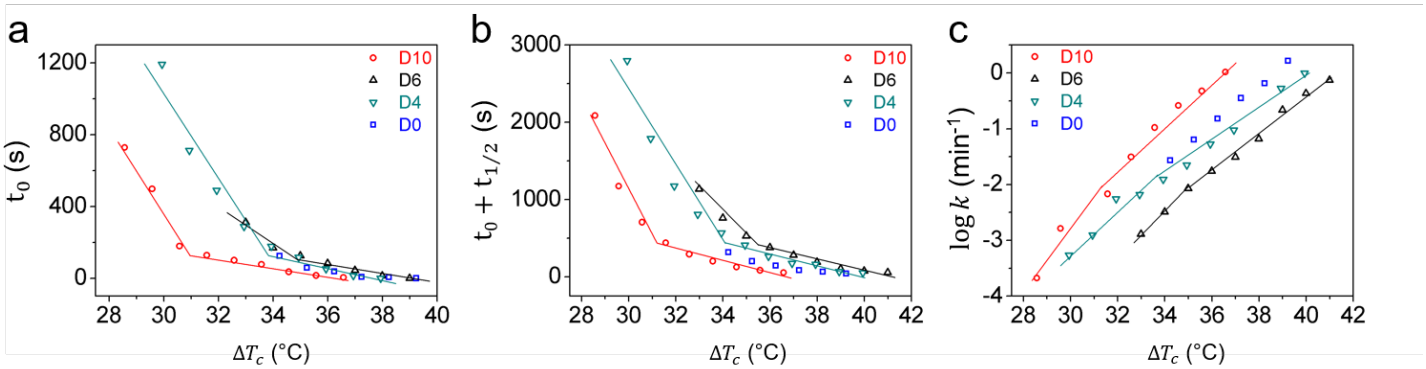

Figure 8. (a) Induction time t_0, (b) half crystallization time $t_0 + t_{1/2}$, and (c) log k for selectively deuterated PCLs after isothermal crystallization at various supercooling temperature ΔT_c.

The crystallization kinetics was further investigated at the same supercooling temperature $\Delta T_c = T_m^0 - T_c$. The curves of t_0, $t_0 + t_{1/2}$, and $log\ k$ plotted against ΔT_c are shown in Figure 8, which display a common deflection point for selectively deuterated PCLs (the deflection point of D0 PCL was skipped here as it has been well studied before[23]). The deflection point indicates the existence of two crystallization regimes, which can be attributed to the interplay between the rate of surface spreading and the rate of secondary nucleation according to the Hoffman-Lauritzen nucleation theory.[24] Furthermore, crystallization rate generally exhibits a relationship of k(D10) > k(D0) > k(D4) > k(D6) at the same ΔT_c.

Analysis of the melting temperature relationship

We propose a mechanism to interpret the melting temperature relationship of PCLs: T_m(D0) > T_m(D6) > T_m(D4) > T_m(D10). Bates et al. reported that the T_m depression of deuterated nonpolar polymers can be attributed to a weaker intermolecular attractive interaction (i.e., London dispersion forces), which is caused by the slightly shorter C-D bond than C-H bond and the corresponding decrease in the polarizability of molecules.[13] Accordingly, one would expect that the T_m of PCLs decreases monotonically with the increase of deuterium content. Nevertheless, the higher T_m value of D6 than D4 suggests that there might be another factor contributing to the melting temperature of PCLs, which is associated with the deuteration sites. Our previous study[6] revealed a weak hydrogen (H) -bond like interaction between the O atom (in the carbonyl group, C=O) and three nearby H atoms (from neighboring chains), due to the larger electronegativity of C than H.[25] This weak H-bond like interaction is

illustrated in Figure 9 for D0, D4, D6, and D10, respectively, which functions as another attractive force that can hold the PCL chains together. The weak H-bond like interaction is an extra force that can hold the PCL chains together. Therefore, substituted the associated H atoms by D atoms may reduce this type of interaction and lower the melting temperature. For the D4 with four D atoms near ester group, two H-bond-like interactions can be affected by the deuteration. While for the D6 that are hexa- deuterated at the 4-, 5-, and 6- positions, only one H-bond-like interaction is affected by deuteration. We expect that the weaker attraction in D4 than D6 from the difference between deuteration sites could lead to an unusual depression of T_m in D4.

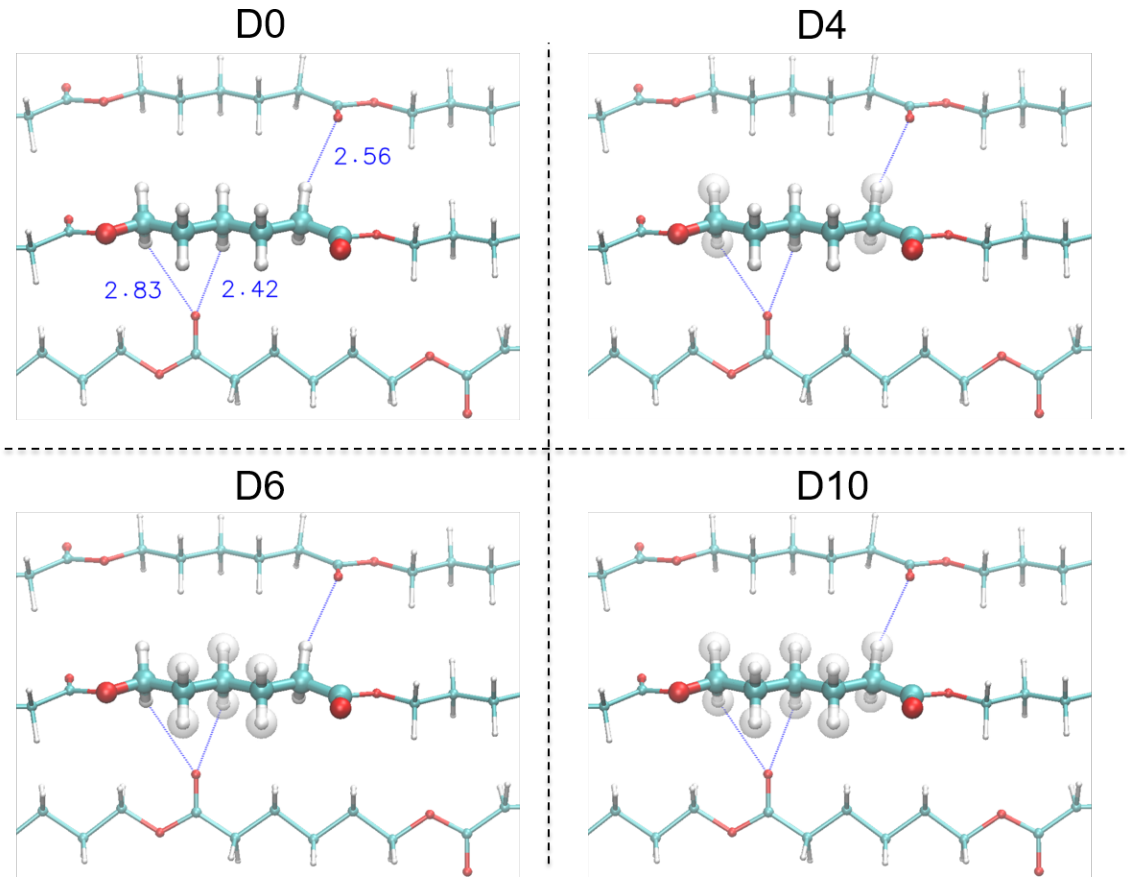

Figure 9. Side view of three PCL chains taken from the cluster model of D0, D4, D6, and D10. Blue dotted lines have the distance of 2.42, 2.56, and 2.83 Å in D0, representing the weak H-bonds. The number for D4, D6, and D10 could be slightly different.

CONCLUSIONS

A series of selectively deuterated PCLs with controlled deuteration sites were synthesized and physical properties were investigated. Crystal morphology and lattice in selectively deuterated PCLs were found to be similar by using SANS measurement. DSC measurement show that the T_m and T_c value decreases with increasing deuterium content except for PCL-D4 which showed an unusual depression. The equilibrium melting temperature T_m^0 of PCLs were extracted through fitting the modified Hoffman-Weeks method and the trend of the value were found to agree well with the T_m data as T_m(D0) > T_m(D6) > T_m(D4) > T_m(D10). Comparatively, D4 exhibited an unusual melting temperature suppression compared to D6. We attributed this non-monotonic trend to the different changes in the weak hydrogen-bond like intermolecular interaction, which is associated with the deuteration sites in the PCLs.

The Avrami model was used to analyze various crystallization kinetics. At the same crystallization temperature T_c, the induction time and half crystallization time were found to change systematically in D0/D10 blends, while among the selectively deuterated PCLs, as same as the T_c value, D4 showed the slowest kinetics. In the meantime, the D0 and D10 samples showed an Avrami index n close to 3, whereas the D4 and D6 samples have n near 2, suggesting a different manner of partially deuterated PCLs. The crystallization kinetics was further analyzed at the same supercooling temperature ΔT_c, the existence of two regimes were revealed and PCLs showed a crystallization kinetics order of k(D10) > k(D0) > k(D4) > k(D6). These results suggest that the crystallization kinetics is sensitive to the nature of the deuteration sites and the crystallization kinetics of partially deuterated PCLs do not always show D content dependence.

Overall, our study provided useful information regarding isotope effects on selectively deuterated PCLs, indicating the necessity of considering the melting temperature and crystallization kinetics differences when deploying fully or selectively deuterated labeling techniques to study the crystal behavior of semi-crystalline polymers. We note that the presented new finding may not be limited to PCLs, but also apply to other types of deuterated polymers with ester group. Nevertheless, the detailed deuteration effects in those systems remain to be explored.

Acknowledgement

The authors gratefully appreciate the support of the National Natural Science Foundation of China (NO. 51573063). L. Li thanks the Chinese Scholarship Council for its financial support. The polymers were synthesized and characterized at the Center for Nanophase Materials Sciences (CNMS) at the Oak Ridge National Laboratory (ORNL), which is a DOE Office of Science User Facility. Neutron scattering studies were performed at the CG-3 Bio-SANS instrument at the High-Flux Isotope Reactor (HFIR), ORNL, which is sponsored by the Office of Biological and Environmental Research, and the Scientific User Facilities Division, Office of Basic Energy Sciences, U.S. Department of Energy. We thank Dr. Jingsong Huang, Dr. Jacek Jakowski, and Dr. Monojoy Goswami (Computational Sciences and Engineering Division, ORNL) for helping with the theoretical analysis.

Supporting information

Synthesis procedure for ε-caprolactone-d_6 and D6-PCL (Figure S1); ^{13}C NMR data and structure for D0, D4, D6 and D10 samples (Figure S2); Crystallization parameters at different crystallization temperature T_c (Table S1).

Reference

1. Knauer, K. M.; Pollino, J.; Schwartz, J.; Moore, L. M.; Morgan, S. E., Surface and interfacial segregation of polyethersulfone deuterated chain ends determined by neutron reflectivity. *Journal of Polymer Science Part B: Polymer Physics* 2017, 55, 293-301.
2. Chen, X.; López-Barrón, C.; Zeng, Y.; Alamo, R. G., Concentration fluctuations in the early stages of LLPS and partial dissolution of melt-memory in broadly distributed ethylene copolymers. *Polymer* 2018, 148, 181-190.
3. Chen, X.; Wignall, G. D.; He, L.; Lopez-Barron, C.; Alamo, R. G., SANS Evidence of Liquid–Liquid Phase Separation Leading to Inversion of Crystallization Rate of Broadly Distributed Random Ethylene Copolymers. *Macromolecules* 2017, 50, 4406-4414.
4. Yang, H.; Liu, D.; Ju, J.; Li, J.; Wang, Z.; Yan, G.; Ji, Y.; Zhang, W.; Sun, G.; Li, L., Chain Deformation on the Formation of Shish Nuclei under Extension Flow: An in Situ SANS and SAXS Study. *Macromolecules* 2016, 49, 9080-9088.
5. López-Barrón, C. R.; Zeng, Y.; Schaefer, J. J.; Eberle, A. P.; Lodge, T. P.; Bates, F. S., Molecular Alignment in Polyethylene during Cold Drawing Using In-Situ SANS and Raman Spectroscopy. *Macromolecules* 2017, 50, 3627-3636.
6. Chang, D.; Li, T.; Li, L.; Jakowski, J.; Huang, J.; Keum, J. K.; Lee, B.; Bonnesen, P. V.; Zhou, M.; Garashchuk, S.; Sumpter, B. G.; Hong, K., Selectively Deuterated Poly(ε-caprolactone)s: Synthesis and Isotope Effects on the Crystal Structures and Properties. *Macromolecules* 2018, 51, 9393-9404.
7. Habersberger, B. M.; Baugh, D. W., Solvent and Polymer Stereochemistry Play Key Roles in Deuterium Exchange and Partial Racemization of Polypropylenes. *Macromolecules* 2018, 51, 1290-1295.
8. Zeng, Y.; López-Barrón, C. R.; Kang, S.; Eberle, A. P. R.; Lodge, T. P.; Bates, F. S., Effect of Branching and Molecular Weight on Heterogeneous Catalytic Deuterium Exchange in Polyolefins. *Macromolecules* 2017, 50, 6849-6860.
9. Kang, S.; Zeng, Y.; Lodge, T. P.; Bates, F. S.; Brant, P.; López-Barrón, C. R., Impact of molecular weight and comonomer content on catalytic hydrogen-deuterium exchange in polyolefins. *Polymer* 2016, 102, 99-105.
10. Wignall, G. D.; Melnichenko, Y. B., Recent applications of small-angle neutron scattering in strongly interacting soft condensed matter. *Reports on Progress in Physics* 2005, 68, 1761.
11. Wignall, G. D., Small angle neutron and x-ray scattering. *Physical Properties of Polymers Handbook* 2007, 407-420.
12. Stehling, F. C.; Ergos, E.; Mandelkern, L., Phase Separation in n-Hexatriacontane-n-Hexatriacontane-d74 and Polyethylene-Poly(ethylene-d4) Systems. *Macromolecules* 1971, 4, 672-677.
13. Bates, F.; Keith, H.; McWhan, D., Isotope effect on the melting temperature of nonpolar polymers. *Macromolecules* 1987, 20, 3065-3070.
14. Reddy, K. R.; Tashiro, K.; Sakurai, T.; Yamaguchi, N., Isotope effect on the isothermal crystallization behavior of isotactic polypropylene blends between the deuterated and hydrogenated species. *Macromolecules* 2009, 42, 1672-1678.
15. Kummara, S.; Tashiro, K.; Monma, T.; Horita, K., Isotope Effect on the Melt–Isothermal Crystallization of Polyoxymethylene D/H Random Copolymers and D/H Blend Samples. *Macromolecules* 2015, 48, 8070-8081.
16. Jakowski, J.; Huang, J.; Garashchuk, S.; Luo, Y.; Hong, K.; Keum, J.; Sumpter, B. G., Deuteration as a Means to Tune Crystallinity of Conducting Polymers. *The Journal of Physical Chemistry Letters* 2017, 8, 4333-4340.
17. Núñez, E.; Ferrando, C.; Malmström, E.; Claesson, H.; Werner, P. E.; Gedde, U. W., Crystal structure, melting behaviour and equilibrium melting point of star polyesters with crystallisable poly(ε-caprolactone) arms. *Polymer* 2004, 45, 5251-5263.
18. Tamaño-Machiavello, M. N.; Costa, C. M.; Romero-Colomer, F. J.; María Meseguer Dueñas, J.; Lanceros-Mendez, S.; Luis Gómez Ribelles, J., Crystallization kinetics of poly (ethylene oxide) confined in semicrystalline poly (vinylidene) fluoride. *Journal of Polymer Science Part B: Polymer Physics* 2018, 56, 588-597.
19. Narayanan, G.; Caydamli, Y.; Tekinalp, H.; Matai, I.; Boy, R.; Chung, C. C.; Shen, J.; Gupta, B. S.; Tonelli, A. E., Thermal, mechanical, and topographical evaluation of nonstoichiometric α-cyclodextrin/poly (ε-caprolactone) pseudorotaxane nucleated poly (ε-caprolactone) composite films. *Journal of Polymer Science Part B: Polymer Physics* 2018, 56, 1529-1537.
20. Avrami, M., Kinetics of Phase Change. I General Theory. *The Journal of chemical physics* 1939, 7, 1103-1112.

21. Avrami, M., Kinetics of Phase Change. II Transformation-Time Relations for Random Distribution of Nuclei. *The Journal of chemical physics* 1940, 8, 212-224.
22. Avrami, M., Granulation, Phase Change, and Microstructure Kinetics of Phase Change. III. *The Journal of chemical physics* 1941, 9, 177-184.
23. Phillips, P. J.; Rensch, G. J.; Taylor, K. D., Crystallization studies of poly (ε-caprolactone). I. Morphology and kinetics. *Journal of Polymer Science Part B: Polymer Physics* 1987, 25, 1725-1740.
24. Huang, C.-L.; Jiao, L.; Zeng, J.-B.; Zhang, M.; Xiao, L.-P.; Yang, K.-K.; Wang, Y.-Z., Crystallization behavior and morphology of double crystalline poly(butylene succinate)-poly(ethylene glycol) multiblock copolymers. *Polymer* 2012, 53, 3780-3790.
25. Sato, H.; Nakamura, M.; Padermshoke, A.; Yamaguchi, H.; Terauchi, H.; Ekgasit, S.; Noda, I.; Ozaki, Y., Thermal Behavior and Molecular Interaction of Poly(3-hydroxybutyrate-co-3-hydroxyhexanoate) Studied by Wide-Angle X-ray Diffraction. *Macromolecules* 2004, 37, 3763-3769.